

Search for  ${}^7\text{H}$  in  ${}^2\text{H}+{}^8\text{He}$  collisions

E. Yu. Nikolskii,<sup>1,\*</sup> A. A. Korshennikov,<sup>1,2</sup> H. Otsu,<sup>1</sup> H. Suzuki,<sup>3</sup> K. Yoneda,<sup>1</sup> H. Baba,<sup>1</sup> K. Yamada,<sup>1</sup> Y. Kondo,<sup>4</sup> N. Aoi,<sup>1</sup> A. S. Denikin,<sup>5,6</sup> M. S. Golovkov,<sup>5</sup> A. S. Fomichev,<sup>5</sup> S. A. Krupko,<sup>5</sup> M. Kurokawa,<sup>1</sup> E. A. Kuzmin,<sup>2</sup> I. Martel,<sup>7</sup> W. Mittig,<sup>8</sup> T. Motobayashi,<sup>1</sup> T. Nakamura,<sup>4</sup> M. Niikura,<sup>9</sup> S. Nishimura,<sup>1</sup> A. A. Ogloblin,<sup>2</sup> P. Roussel-Chomaz,<sup>8</sup> A. Sanchez-Benitez,<sup>7</sup> Y. Satou,<sup>4</sup> S. I. Sidorchuk,<sup>5</sup> T. Suda,<sup>1</sup> S. Takeuchi,<sup>1</sup> K. Tanaka,<sup>1</sup> G. M. Ter-Akopian,<sup>5</sup> Y. Togano,<sup>10</sup> and M. Yamaguchi<sup>1</sup>

<sup>1</sup>RIKEN Nishina Center, Hirosawa 2-1, Wako, Saitama 351-0198, Japan

<sup>2</sup>RRC Kurchatov Institute, Kurchatov Square 1, RU-123182 Moscow, Russia

<sup>3</sup>Department of Physics, University of Tokyo, Tokyo 113-0033, Japan

<sup>4</sup>Department of Physics, Tokyo Institute of Technology, 2-12-1 Ookayama, Meguro-ku, Tokyo 152-8550, Japan

<sup>5</sup>Flerov Laboratory of Nuclear Reactions, JINR, RU-141980 Dubna, Moscow Region, Russia

<sup>6</sup>Department of Nuclear Physics, International University "Dubna", RU-141980 Dubna, Moscow Region, Russia

<sup>7</sup>Departamento de Fisica Aplicada, Universidad de Huelva, ES-21071 Huelva, Spain

<sup>8</sup>GANIL, BP 55027, F-14076 Caen Cedex 05, France

<sup>9</sup>Center for Nuclear Study (CNS), University of Tokyo, Wako, Saitama 351-0198, Japan

<sup>10</sup>Department of Physics, Rikkyo University, Tokyo 171-8501, Japan

(Received 28 February 2009; revised manuscript received 23 April 2010; published 16 June 2010)

An experimental search for the low-lying  ${}^7\text{H}$  resonance was performed with the  ${}^2\text{H}({}^8\text{He}, {}^3\text{He}){}^7\text{H}$  reaction studied at forward center-of-mass angles ( $6^\circ$ – $14^\circ$ ) with a 42 A MeV  ${}^8\text{He}$  beam. No well-pronounced peak of  ${}^7\text{H}$  was observed; however, the obtained spectrum was found to have a peculiarity at  $\sim 2$  MeV above the  $t + 4n$  threshold. The data allow us to set a c.m.s. cross section level of  $\sim 30$   $\mu\text{b}/\text{sr}$  for the low-energy part of the  ${}^7\text{H}$  spectrum. The test reaction  ${}^2\text{H}({}^{12}\text{Be}, {}^3\text{He}){}^{11}\text{Li}$ , involving the same one-proton ( $d, {}^3\text{He}$ ) transfer, was studied simultaneously on a 71 A MeV satellite beam where a cross section of  $\simeq 1$  mb/sr was measured for the population of the  ${}^{11}\text{Li}$  ground state.

DOI: [10.1103/PhysRevC.81.064606](https://doi.org/10.1103/PhysRevC.81.064606)

PACS number(s): 27.20.+n, 25.60.Je

## I. INTRODUCTION

Investigation of exotic nuclei near and beyond the drip lines has become a major subject in nuclear structure physics resulting in the discovery of new phenomena like halos, skins, shell quenching, and the appearance of new magic numbers. The region of light neutron-rich nuclei is especially interesting, since nuclear matter can be explored here under extreme conditions and the stability limits can be reached by “adding” only a few neutrons to the stable isotopes. Also, the search for and/or the study of resonance states in the light, very neutron-rich nuclear systems represents one of the most effective ways to test modern theoretical models, which are aiming to describe the nuclear stability and structure, but which are mainly based on the properties of bound nuclear matter. In this connection, the exotic superheavy hydrogen  ${}^7\text{H}$ , having an extreme neutron to proton ratio  $N/Z = 6$ , attracts special attention.

The first theoretical estimation of the stability of  ${}^7\text{H}$  made by Baz’ *et al.* [1] showed that this nucleus may even be bound. However, in numerous measurements using the  $\Delta E$ - $E$  method, no indication for the hyperbola of the bound  ${}^7\text{H}$ , which could be produced in different reactions, was observed. Also, early experiments, which aimed at the search for a quasistable  ${}^7\text{H}$  in the  ${}^7\text{Li}(\pi^-, \pi^+)$  reaction [2,3] and bound  ${}^7\text{H}$  nucleus in the spontaneous fission of  ${}^{252}\text{Cf}$  [4], were unsuccessful. One further attempt to detect a long-lived state

of  ${}^7\text{H}$ , populated in the  ${}^2\text{H}({}^8\text{He}, {}^7\text{H})$  reaction, could give only upper limits of 3 nb/sr and 1 ns for the reaction cross section and  ${}^7\text{H}$  lifetime, respectively [5].

The observation of a low-lying resonance state of  ${}^5\text{H}$  [6,7] intensified interest in this issue, allowing one to speculate about the existence of an unbound  ${}^7\text{H}$  state near the  $t + 4n$  threshold. Below, we briefly discuss the current theoretical and experimental works dedicated to the  ${}^7\text{H}$  resonance.

Calculations within the seven-body hyperspherical functions method [8] predict that  ${}^7\text{H}$  is unbound by  $\simeq 0.9$  MeV with respect to the  $t + 4n$  threshold. The total binding energy of  ${}^7\text{H}$  was estimated in Ref. [9] to be  $\sim 5.4$  MeV, implying that the ground state (g.s.) of this nucleus is located about 3 MeV above the  $t + 4n$  threshold. The antisymmetrized molecular dynamics (AMD) approach gives a value of  $\sim 7$  MeV for the  ${}^7\text{H}(t + 4n)$  resonance energy [10]. Very recently, the same authors presented new results on the  ${}^7\text{H}$  ground state, studied by the AMD triple-S method [11]. The calculations show significant mixing of dineutron ( $t + {}^2n + {}^2n$ ) components with a spatially extended distribution and the estimated energy of  ${}^7\text{H}$  is about 4 MeV. Questions arising about the width of the  ${}^7\text{H}$  resonance are also very important. In Ref. [9], it was stressed that  ${}^7\text{H}$  should undergo the unique five-body decay into  $t + 4n$  and its width may be very narrow. Some theoretical estimations of the  ${}^7\text{H}$  width show that for a decay energy  $E \leq 3$  MeV one can expect a state with  $\Gamma \leq 1$  MeV [5].

The first experimental evidence for the existence of the  ${}^7\text{H}$  state was observed in the  ${}^1\text{H}({}^8\text{He}, pp){}^7\text{H}$  reaction [9]. The missing-mass spectrum for  ${}^7\text{H}$  obtained in that work demonstrates a very sharp increase starting from the  $t + 4n$

\*On leave from RRC Kurchatov Institute, Moscow, Russia; nikolski@ribf.riken.jp

threshold. However, this interesting finding did not allow the authors to give quantitative information about the parameters of the resonance. Stopped  $\pi^-$ -meson absorption in  $^9\text{Be}$  and  $^{11}\text{B}$  targets was recently studied in Ref. [12] where some peculiarity in the spectrum near the threshold was found in the  $^{11}\text{B}(\pi^-, p^3\text{He})^7\text{H}$  reaction, but no evidence for the low-lying  $^7\text{H}$  state was observed in the  $^9\text{Be}(\pi^-, pp)^7\text{H}$  channel. Very recently, the question of the  $^7\text{H}$  existence was investigated via the use of the transfer reaction  $^{12}\text{C}(^8\text{He}, ^{13}\text{N})^7\text{H}$  [13]. Although the authors could attribute only seven events to this reaction channel, the observation of a very narrow  $^7\text{H}$  resonance, lying at less than 1 MeV above the  $t + 4n$  threshold, was claimed. Lack of statistics in the spectrum only allowed the authors of Ref. [14] to place a limit on the cross section for the formation of  $^7\text{H}$  near the threshold in the  $^2\text{H}(^8\text{He}, ^3\text{He})^7\text{H}$  reaction. The authors of Ref. [15] investigated the same reaction and came to the conclusion that there was some evidence in the measured missing-mass spectrum for the observation of a  $^7\text{H}$  at  $\sim 2$  MeV, but their experimental acceptance covered only a few MeV of the full  $^7\text{H}$  energy range.

In this article, we report on the experimental search for a  $^7\text{H}$  state populated in the  $^2\text{H}(^8\text{He}, ^3\text{He})^7\text{H}$  reaction. The simplicity of the one-proton pickup ( $d, ^3\text{He}$ ) reaction mechanism, measurements performed at extreme forward angles (where the reaction cross section should be at its largest), and the use of a high-intensity  $^8\text{He}$  beam gave a good opportunity to populate the ground state of  $^7\text{H}$  with reasonable statistics.

## II. EXPERIMENTAL SETUP

The experiment was performed at the projectile-fragment separator RIPS [16], which is part of the RIBF accelerator complex operated by RIKEN Nishina Center and Center for Nuclear Study, University of Tokyo. A primary  $^{18}\text{O}$  beam with energy 100 A MeV and intensity of  $\sim 500$  particle nA bombarded a  $^9\text{Be}$  target with a thickness of 12 mm. The secondary beam consisted of a cocktail of  $^8\text{He}$  and  $^{12}\text{Be}$  with average energies of 42 and 71 A MeV, and intensities of  $1.4 \times 10^5$  and  $2.6 \times 10^5$  pps, respectively. A cryogenic target cell was used, supplied with 6.5- $\mu\text{m}$  Havar windows, and filled with deuterium gas at 30 K and a pressure of 0.5 atm. This resulted in a target thickness of  $2.4 \times 10^{20}$  deuterons/cm $^2$ . The beam energy and parameters of the detection system were optimized by utilizing the results obtained in complete Monte-Carlo simulations preceding the experiment. The presence of  $^{12}\text{Be}$  nuclei in the beam enabled us to study the  $^2\text{H}(^{12}\text{Be}, ^3\text{He})^{11}\text{Li}$  reaction, as discussed later in this article.

The experimental setup is shown in Fig. 1. Two plastic scintillators were used to identify each particle in the secondary beam and to measure their energies by the time of flight. The trajectories of individual projectiles were measured by a pair of multiwire proportional chambers (MWPCs). Recoiling particles (e.g.,  $^3\text{He}$  or tritons) were detected by the RIKEN telescope of silicon strip detectors with an additional  $\Delta E$  array of six thin ( $\simeq 40$   $\mu\text{m}$ ) Si strip counters. The RIKEN telescope consisted of a 250- $\mu\text{m}$  double-sided strip detector (DSD) and six 750- $\mu\text{m}$  single-sided sector detectors (SSD). The SSDs were used to measure the reaction channels with high-energy recoil particles, for example, the  $^6\text{Li}$  nuclei from

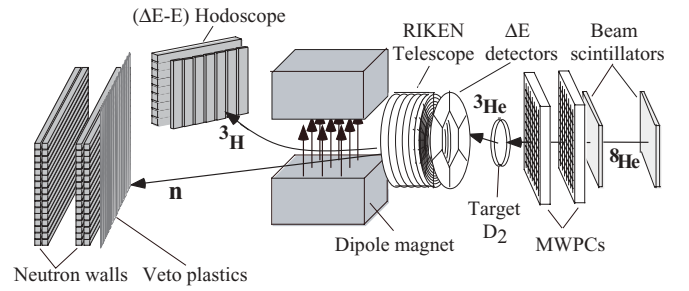


FIG. 1. Experimental setup.

the  $^2\text{H}(^8\text{He}, ^6\text{Li})4n$  reaction. This telescope provided particle identification, energy measurements, and hit positions of the detected reaction products. By taking the known input positions and angles of the projectile nuclei on the target, the reaction angles of the products could be defined.

The beam passed through the central hole in the telescope. Projectile-like particles from breakup channels (e.g., tritons and neutrons from the  $^7\text{H} \rightarrow t + 4n$  decay) were measured by a downstream detection system consisting of a dipole magnet, a  $\Delta E(1\text{ cm})$ - $E(6\text{ cm})$  hodoscope of plastic scintillators, and a four-layer neutron hodoscope array. A thin layer of plastic scintillators was installed in front of the neutron array to reject events from charged particles.

## III. RESULTS

### A. $^2\text{H}(^8\text{He}, t)^7\text{He}$ reaction

To experimentally determine the missing-mass resolution and verify the time stability of the detectors, the  $^2\text{H}(^8\text{He}, t)^7\text{He}$  reaction was used as a reference. In Fig. 2(a), the inclusive triton spectrum from the  $^2\text{H}(^8\text{He}, t)$  reaction and the spectrum of tritons detected in coincidence with  $^6\text{He}$  in the hodoscope [Fig. 2(b)] are shown as a function of the  $^7\text{He}$  energy above the  $^6\text{He} + n$  threshold. The gray histograms show the normalized background measured with an empty target. The strongest peaks in Figs. 2(a) and 2(b) represent the well-known  $^7\text{He}$  ground state, which is unstable with respect to the  $^6\text{He} + n$  decay with  $E_d \simeq 0.44$  MeV. The width of the peak (FWHM  $\approx 1.7$  MeV) determines the experimental resolution and is close to the Monte-Carlo simulation performed for this reaction, taking into account all experimental conditions (the natural width of  $^7\text{He}_{\text{g.s.}}$  is small,  $\Gamma = 0.16$  MeV). As can be seen in Fig. 2, no excited states of  $^7\text{He}$  were observed. Most probably, the known  $^7\text{He}$  excited state at  $E_{^6\text{He}+n} \simeq 3.3$  MeV [17], which decays mainly into  $^4\text{He} + 3n$ , was not observed here due to low statistics and high background. Its presence could be revealed through coincidences with the  $^4\text{He}$  nuclei produced in the main decay mode of this  $^7\text{He}$  state; however, the downstream detection system had a low acceptance for such  $^4\text{He}$  products. Nevertheless, the common features of the  $^7\text{He}$  spectra presented in Fig. 2 and those measured in Ref. [17] via the  $^1\text{H}(^8\text{He}, d)^7\text{He}$  reaction are quite similar.

### B. $^2\text{H}(^8\text{He}, ^3\text{He})^7\text{H}$ reaction

It is well known that nucleon transfer is a dominant reaction mechanism in nucleus-nucleus collisions at energies

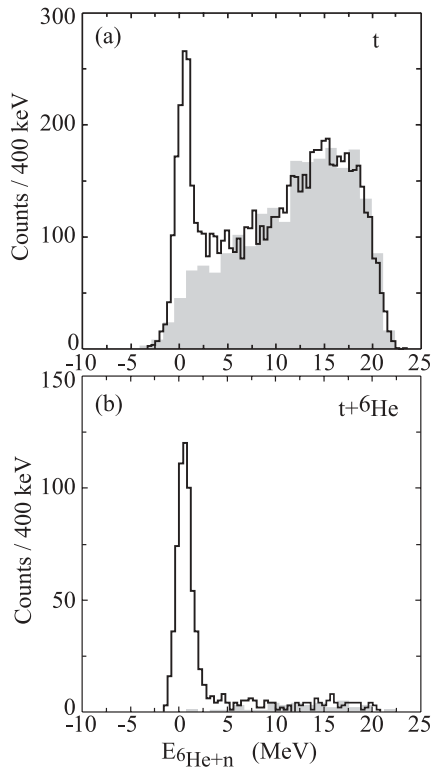


FIG. 2. Missing-mass spectra of  ${}^7\text{He}$  from the reactions (a)  ${}^2\text{H}({}^8\text{He},t)$  and (b)  ${}^2\text{H}({}^8\text{He},t{}^6\text{He})$ . The gray histograms represent the empty-target background.

of a few tens of MeV/nucleon. Therefore, as was mentioned in the Introduction, one might expect that the simple one-proton pickup ( $d, {}^3\text{He}$ ) reaction on  ${}^8\text{He}$  measured at small center-of-mass angles should provide a sensitive tool to search for an exotic low-lying resonance state of  ${}^7\text{H}$ .

In Fig. 3(c), the  ${}^7\text{H}$  missing-mass spectrum from the reaction  ${}^2\text{H}({}^8\text{He}, {}^3\text{He}){}^7\text{H}$  is presented. The spectrum was formed from the energy and trajectory data of the  ${}^3\text{He}$  recoils detected in coincidence with tritons from the decay of the residual  ${}^7\text{H}$  system. The spectrum is shown as a function of the  ${}^7\text{H}$  energy above the  $t + 4n$  threshold. The gray histogram represents the normalized background data obtained from the empty-target measurement. The inclusive  ${}^7\text{H}$  missing-mass spectrum obtained without applying the triton coincidence condition [see Fig. 3(a)] demonstrates a very high background level, which mainly comes from the target cell windows. As one can see, the coincidence requirement dramatically reduces the number of background events (by more than 100 times), resulting in a signal-to-background ratio of better than 10 at low  ${}^7\text{H}$  energies. This allows one to effectively select the  ${}^2\text{H}({}^8\text{He}, {}^3\text{He}){}^7\text{H}$  reaction channel from the other, numerous processes. The solid and dashed curves (Curves 1 and 2, respectively) in Fig. 3(c) show the nonresonant continuum distributions from calculations of five-body ( $t + n + n + n + n$ ) and three-body ( $t + {}^2n + {}^2n$ ) phase volumes, respectively. In the calculations, the detection efficiency inherent to the  ${}^3\text{He}-t$  coincidence measurements [see Fig. 3(b)] and the experimental resolution in this reaction channel (FWHM  $\approx 1.9$  MeV) were taken into account. The curves are normalized to the experimental  ${}^7\text{H}$

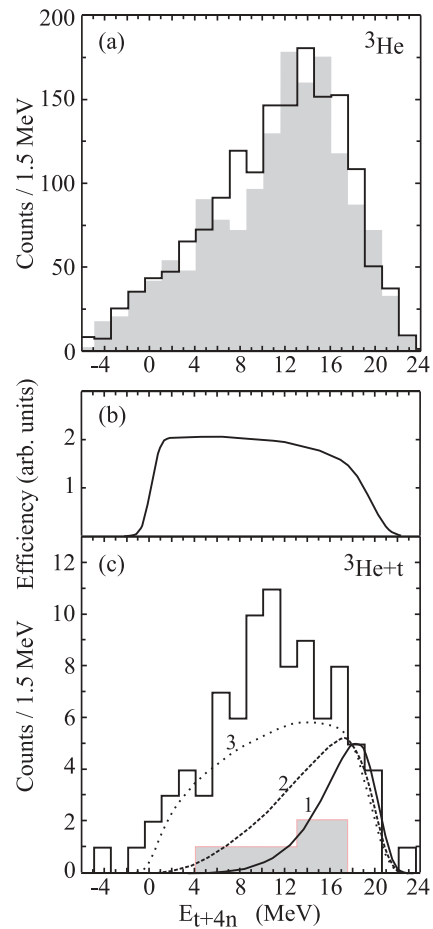


FIG. 3. Missing-mass spectra of  ${}^7\text{H}$  from the reaction  ${}^2\text{H}({}^8\text{He}, {}^3\text{He})$ : (a) without coincidence with tritons, (b) detection efficiency in arbitrary units, and (c) in coincidence with tritons. The spectra are shown relative to the  $t + 4n$  threshold. The gray histograms show the empty-target background. The curves 1, 2, and 3 represent nonresonant continuums. See text for details.

spectrum at  $E_{t+4n} = 18$  MeV. Curve 2 can be considered as an extreme case where the relative motion in both neutron pairs is described by a  $\delta$  function. We note that other distributions, which were calculated by taking the final state interactions in the  $(t + n)$  and  $(n + n)$  subsystems into account, were found to lie between Curves 1 and 2. Figure 3(c) shows the most extreme, unrealistic case of the two-body ( $t + {}^4n$ ) phase volume distribution (dotted; Curve 3), implying the motion of a triton and tetra-neutron with zero binding energy.

Despite the low number of accumulated statistics, some remarkable features inherent to the missing-mass spectrum in Fig. 3(c) should be noted. No clear evidence for a  ${}^7\text{H}$  peak is seen at low energies; however, close to  $E_{t+4n} = 0$  MeV, the experimental spectrum is much steeper than that of Curve 2, which is an extreme case. Furthermore, below 5 MeV, the spectrum exhibits a “shoulder” centered at  $\sim 2$  MeV. One could say that the low-energy part of the spectrum looks similar to that of Curve 3, which assumes the existence of a hypothetical quasisubbound tetra-neutron. However, the explanation of a peculiar threshold behavior in the missing-mass spectrum of  ${}^7\text{H}$  seems unrealistic due to the lack of any reliable experimental proofs,

suggesting that any bound or narrow quasibound  ${}^4n$  state exists. Modern theoretical approaches [18,19] do not predict a  ${}^4n$  nucleus either. Therefore, it is justified to regard the observed shape of the experimental spectrum near the  $t + 4n$  threshold as an indication of a  ${}^7\text{H}$  state. The reaction cross section of the  ${}^7\text{H}$  production in the low-energy region is determined to be  $\sim 5 \mu\text{b}/\text{sr}$  per unit count in the spectrum within the angular range of  $\simeq 6^\circ\text{--}14^\circ$  in the center-of-mass system.

Although the experimental spectrum of  ${}^7\text{H}$  obtained in the  ${}^2\text{H}({}^8\text{He}, {}^3\text{He}){}^7\text{H}$  reaction [see Fig. 3(c)] does not exhibit such a sharp rise just above the threshold as what was observed in the  ${}^1\text{H}({}^8\text{He}, pp){}^7\text{H}$  reaction [9], it demonstrates a specific behavior at low energy that cannot be reproduced with reasonable assumptions concerning the phase space. This leads us to the conclusion that the result obtained in this experiment provides one further piece of evidence for the possible existence of a low-lying  ${}^7\text{H}$  resonance. The noted difference in the shapes of the  ${}^7\text{H}$  spectra could reflect peculiarities in the mechanisms of the  $(d, {}^3\text{He})$  and  $(p, pp)$  reactions exploited here and in Ref. [9] with the use of  ${}^8\text{He}$  beams at energies of 42 and 61 A MeV, respectively. Both results provide some evidence that the energy and width of this state are larger than the values reported in Ref. [13] for the  ${}^7\text{H}$  ground-state resonance. One should note, however, that the manifestation of several overlapping resonances near the threshold cannot be excluded.

The spectrum in Fig. 3(c) shows an apparent maximum at about 10.5 MeV; the origin of this is unclear. Nevertheless, we do not exclude the possibility that it might be the manifestation of a  ${}^7\text{H}$  excitation continuum with energy centered around 10.5 MeV.

### C. ${}^2\text{H}({}^{12}\text{Be}, {}^3\text{He}){}^{11}\text{Li}$ reaction

To check the reliability of the obtained experimental data and the effectiveness of the chosen  $(d, {}^3\text{He})$  reaction in the population of lowest states of exotic, weakly bound nuclei, the same reaction was studied with  ${}^{12}\text{Be}$  projectiles. The excitation spectrum of  ${}^{11}\text{Li}$ , produced in the one-proton  $(d, {}^3\text{He})$  transfer, was extracted from the data on  ${}^3\text{He}$  recoils emitted from the target following the passage of the  ${}^{12}\text{Be}$  nuclei that were presented in the cocktail beam. The  ${}^{11}\text{Li}$  spectrum obtained from the  ${}^2\text{H}({}^{12}\text{Be}, {}^3\text{He}){}^{11}\text{Li}$  reaction is shown in Fig. 4. The solid histogram in Fig. 4 shows a well-pronounced peak corresponding to the ground state of  ${}^{11}\text{Li}$ , which can clearly be identified above the structureless gray histogram that represents the normalized background. The part of the spectrum on the right of the  ${}^{11}\text{Li}_{\text{g.s.}}$  peak, that is, that exceeding the background, most likely reflects the population of (unresolved here)  ${}^{11}\text{Li}$  excited states reported earlier [20–25]. A cross-section value of  $\sim 1 \text{ mb}/\text{sr}$  was deduced for the  ${}^{11}\text{Li}$  ground state from these data. This value is about 30 times larger than the population cross section of  ${}^7\text{H}$ , obtained for the group of events near 2 MeV excitation energy. Such a large difference in the cross sections could possibly be explained by the reduction effect [6] caused by scattering on the valence neutrons of  ${}^8\text{He}$ . In Ref. [6], the measured cross section for a similar transfer reaction,  ${}^1\text{H}({}^6\text{He}, {}^2\text{He}){}^5\text{H}$ , was found to be about 1 order of magnitude less than the results of DWBA calculations. Estimations based on the known  $(d + n)$

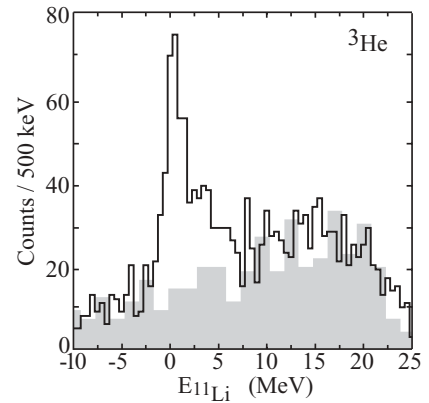


FIG. 4. Spectrum of  ${}^{11}\text{Li}$  from the reaction  ${}^2\text{H}({}^{12}\text{Be}, {}^3\text{He})$ . The gray histogram shows the empty-target background.

and  $({}^3\text{He} + n)$  total cross sections and the  ${}^4\text{He}$  and  ${}^8\text{He}$  matter radii also lead to a value of 1 order of magnitude for the reduction factor of the  ${}^2\text{H}({}^8\text{He}, {}^3\text{He}){}^7\text{H}$  reaction cross section.

## IV. CROSS SECTIONS

The data allow us to set a value of  $\sim 30 \mu\text{b}/\text{sr}$  on the cross section of the  ${}^2\text{H}({}^8\text{He}, {}^3\text{He}){}^7\text{H}$  reaction channel that populates the low-lying  ${}^7\text{H}$  resonance ( $E_{t+4n} \leq 3 \text{ MeV}$ ) at the beam energy reported here. Similar values,  $\sim 10 \mu\text{b}/\text{sr}/\text{MeV}$  and  $\sim 20 \mu\text{b}/\text{sr}$ , respectively, were reported for the  ${}^1\text{H}({}^8\text{He}, pp){}^7\text{H}$  reaction cross section [9] and cross-section limit achieved for the  ${}^2\text{H}({}^8\text{He}, {}^3\text{He})$  reaction at a beam energy of 25 A MeV [14]. It is clear that the measured cross sections are rather low, in contrast to typical values of a few mb/sr for one-proton transfer reactions at small center-of-mass angles. Besides the reduction effect mentioned earlier, there might be another reason for such low reaction probabilities. It has been shown by recent AMD calculations, performed by Aoyama and Itagaki [11], that the ground state of  ${}^7\text{H}$  has a significant admixture of dineutron components ( $t + {}^2n + {}^2n$ ) with a spatially extended distribution that peaks at  $\sim 6 \text{ fm}$ , much farther than in  ${}^8\text{He}$  ( $\sim 3 \text{ fm}$ ). Therefore, one may expect a small overlap between the initial ( ${}^8\text{He}$ ) and final ( ${}^7\text{H}$ ) wave functions, resulting in a reduction of the reaction cross sections.

It is noted that rather low cross sections were reported for the  ${}^7\text{H}$  production reactions at forward angles, where, in fact, the largest cross section values are expected. The only work that claims the observation of a  ${}^7\text{H}$  resonance is Ref. [13], where a cross section of  $\sim 40 \mu\text{b}/\text{sr}$  was reported for the  ${}^{12}\text{C}({}^8\text{He}, {}^{13}\text{N}){}^7\text{H}$  reaction in which a quite narrow, low-lying  ${}^7\text{H}$  resonance ( $E_R = 0.57_{-0.21}^{+0.42} \text{ MeV}$ ,  $\Gamma = 0.09_{-0.06}^{+0.94} \text{ MeV}$ ) was populated within a wide angular range ( $\theta_{\text{CM}} \simeq 10^\circ\text{--}48^\circ$ ).

To compare the cross section values for the  ${}^7\text{H}$  production obtained in the present work and that reported in Ref. [13], we performed DWBA calculations using the code DWUCK5 [26]. A set of initial parameters of Woods-Saxon optical model potentials was obtained for the  ${}^2\text{H}({}^8\text{He}, {}^3\text{He}){}^7\text{H}$  reaction by fitting data from  ${}^8\text{He}(p, p)$  [22,27–30],  ${}^6\text{Li}(p, p)$ ,  ${}^6\text{Li}(d, d)$ , and  ${}^6\text{Li}({}^3\text{He}, {}^3\text{He})$  [31–33] elastic scattering reactions. The final set of the potential parameters was then fixed to fit the angular distribution of tritons from the reaction  ${}^2\text{H}({}^8\text{He}, t){}^7\text{He}_{\text{g.s.}}$



measured in this experiment. The differential cross section for the  ${}^{12}\text{C}({}^8\text{He}, {}^{13}\text{N}){}^7\text{H}$  reaction was calculated using, for the entrance and exit channels, respectively, the potentials found in Ref. [34] for the  ${}^7\text{Li}(123\text{ MeV}) + {}^{13}\text{C}$  and  ${}^7\text{Be}(84\text{ MeV}) + {}^{14}\text{N}$  systems. In calculations performed for the  ${}^2\text{H}({}^8\text{He}, {}^3\text{He}){}^7\text{H}$  and  ${}^{12}\text{C}({}^8\text{He}, {}^{13}\text{N}){}^7\text{H}$  reactions, a spectroscopic factor of  $\text{SF} = 2$  for the  ${}^8\text{He} = p + {}^7\text{H}(1/2^+)$  clustering was assumed (the upper limit possible for a system with two protons in its core). Other SFs were set as follows:  $\text{SF}[{}^3\text{He} = p + d] = 1.5$  [35] and  $\text{SF}[{}^{13}\text{N} = p + {}^{12}\text{C}] = 0.61$  [36]. Finally, our calculations yielded cross sections of  $\sim 5\text{ mb/sr}$  and  $\sim 70\text{ }\mu\text{b/sr}$  for the  ${}^2\text{H}({}^8\text{He}, {}^3\text{He}){}^7\text{H}$  and  ${}^{12}\text{C}({}^8\text{He}, {}^{13}\text{N}){}^7\text{H}$  reactions, respectively. These are the values averaged over the center-of-mass angular ranges explored in the present work and in Ref. [13]. Since the cross section calculated for the  ${}^{12}\text{C}({}^8\text{He}, {}^{13}\text{N}){}^7\text{H}$  reaction turned out to be about two times larger than the experimental value reported in Ref. [13], it is perhaps reasonable to assume that the spectroscopic factor is a factor of 2 smaller in the case of  $p + {}^7\text{H}$  clustering of  ${}^8\text{He}$ . Thus, for the  ${}^2\text{H}({}^8\text{He}, {}^3\text{He}){}^7\text{H}$  reaction, one may expect a cross section of  $\sim 2.5\text{ mb/sr}$ , which is almost 2 orders of magnitude larger than the cross section determined for this reaction in the present work. One possible explanation for this discrepancy could be that the dynamics inherent to the  $(d, {}^3\text{He})$  and  $({}^{12}\text{C}, {}^{13}\text{N})$  transfers are different and the population of the low-lying resonance in  ${}^7\text{H}$  in the  ${}^2\text{H}({}^8\text{He}, {}^3\text{He})$  reaction is suppressed with respect to the  ${}^{12}\text{C}({}^8\text{He}, {}^{13}\text{N})$  reaction. However, we do not currently know of any rational reason for such a suppression. Thus, according to the performed DWBA calculations, the result obtained in

the present work for the cross section of the  ${}^2\text{H}({}^8\text{He}, {}^3\text{He}){}^7\text{H}$  reaction in the low-energy part of the  ${}^7\text{H}$  spectrum and that reported in Ref. [13] for a narrow  ${}^7\text{H}$  resonance, populated in the  ${}^{12}\text{C}({}^8\text{He}, {}^{13}\text{N}){}^7\text{H}$  reaction, are in conflict with each other.

## V. SUMMARY

We performed an experimental search for the  ${}^7\text{H}$  resonance produced in the  ${}^2\text{H}({}^8\text{He}, {}^3\text{He}){}^7\text{H}$  reaction at a beam energy of 42 A MeV. The observed missing-mass spectrum exhibits a peculiarity at  $\sim 2\text{ MeV}$  that might indicate the population of some low-energy state (or states) of  ${}^7\text{H}$  in this reaction. A cross section level of  $\sim 30\text{ }\mu\text{b/sr}$  for the low-lying  ${}^7\text{H}$  resonance production was estimated. In addition, the  ${}^7\text{H}$  spectrum demonstrates peculiarity at  $\sim 10.5\text{ MeV}$  that could be due to the manifestation of a  ${}^7\text{H}$  excitation continuum. DWBA analysis revealed a discrepancy between the cross sections extracted from the low-lying parts of the  ${}^7\text{H}$  spectra in the present work and Ref. [13]. The reason for the discrepancy is unknown at the present time. Evidently, more experiments are necessary to accumulate a higher number of statistics in the spectrum for  ${}^7\text{H}$ , thus allowing for complete kinematic measurements of its decay products.

## ACKNOWLEDGMENTS

The authors thank Professor M. V. Zhukov for reading the manuscript and his helpful suggestions. We also thank Professor S. B. Sakuta for valuable discussions clarifying the use of the DWBA approach.

- 
- [1] A. I. Baz', V. I. Goldansky, V. Z. Goldberg, and Ya. B. Zeldovich, *Light and Intermediate Nuclei Near the Borders of Nucleon Stability* (Nauka, Moscow, 1972) [in Russian].
- [2] K. K. Seth, CERN Report 81-09-655, Geneva, 1981.
- [3] V. S. Evseev, V. S. Kurbatov, V. M. Sidorov, V. B. Belyaev, J. Wrzecionko, M. Daum, R. Frosch, J. McCulloch, and E. Steiner, *Nucl. Phys. A* **352**, 379 (1981).
- [4] D. V. Aleksandrov, Yu. A. Glukhov, A. S. Dem'yanova, V. I. Dukhanov, I. B. Mazurov, B. G. Novatskiĭ, A. A. Ogloblin, S. B. Sakuta, and D. N. Stepanov, *Sov. J. Nucl. Phys.* **36**, 783 (1982) [*Yad. Fiz.* **36**, 1351 (1982)].
- [5] M. S. Golovkov *et al.*, *Phys. Lett. B* **588**, 163 (2004).
- [6] A. A. Korshennikov *et al.*, *Phys. Rev. Lett.* **87**, 092501 (2001).
- [7] S. I. Sidorchuk *et al.*, *Nucl. Phys. A* **719**, 229c (2003).
- [8] N. K. Timofeyuk, *Phys. Rev. C* **65**, 064306 (2002).
- [9] A. A. Korshennikov *et al.*, *Phys. Rev. Lett.* **90**, 082501 (2003).
- [10] S. Aoyama and N. Itagaki, *Nucl. Phys. A* **738**, 362 (2004).
- [11] S. Aoyama and N. Itagaki, *Phys. Rev. C* **80**, 021304(R) (2009).
- [12] Yu. B. Gurov, B. A. Chernyshev, S. V. Isakov, V. S. Karpukhin, S. V. Lapushkin, I. V. Laukhin, V. A. Pechkurov, N. O. Poroshin, and V. G. Sandukovsky, *Eur. Phys. J. A* **32**, 261 (2007).
- [13] M. Caamaño *et al.*, *Phys. Rev. Lett.* **99**, 062502 (2007).
- [14] G. M. Ter-Akopian *et al.*, *Eur. Phys. J. Spec. Top.* **150**, 61 (2007).
- [15] S. Fortier *et al.*, *AIP Proc.* **912**, 3 (2007).
- [16] T. Kubo, M. Ishihara, N. Inabe, H. Kumagai, I. Tanihata, and K. Yoshida, *Nucl. Instrum. Methods Phys. Res. B* **70**, 309 (1992).
- [17] A. A. Korshennikov *et al.*, *Phys. Rev. Lett.* **82**, 3581 (1999).
- [18] S. C. Pieper, *Phys. Rev. Lett.* **90**, 252501 (2003).
- [19] N. K. Timofeyuk, *J. Phys. G: Nucl. Part. Phys.* **29**, L9 (2003).
- [20] T. Kobayashi, *Nucl. Phys. A* **538**, 343c (1992).
- [21] H. G. Bohlen *et al.*, *Z. Phys. A* **351**, 7 (1995).
- [22] A. A. Korshennikov *et al.*, *Phys. Rev. C* **53**, R537 (1996).
- [23] M. Zinser *et al.*, *Nucl. Phys. A* **619**, 151 (1997).
- [24] M. G. Gornov, Yu. Gurov, S. Lapushkin, P. Morokhov, V. Pechkurov, T. K. Pedlar, Kamal K. Seth, J. Wise, and D. Zhao, *Phys. Rev. Lett.* **81**, 4325 (1998).
- [25] H. Simon *et al.*, *Nucl. Phys. A* **791**, 267 (2007).
- [26] P. D. Kunz, computer code DWUCK5 [<http://spot.colorado.edu/~kunz/DWBA.html>].
- [27] F. Skaza *et al.*, *Phys. Lett. B* **619**, 82 (2005).
- [28] R. Wolski *et al.*, *Nucl. Phys. A* **701**, 29c (2002).
- [29] A. A. Korshennikov *et al.*, *Phys. Lett. B* **343**, 53 (1995).
- [30] A. A. Korshennikov *et al.*, *Phys. Lett. B* **316**, 38 (1993).
- [31] D. Gupta, C. Samanta, and R. Kanungo, *Nucl. Phys. A* **674**, 77 (2000).
- [32] M. Avrigeanu, V. von Oertzen, U. Fischer, and V. Avrigeanu, *Nucl. Phys. A* **759**, 327 (2005).
- [33] T. Sinha, Subinit Roy, and C. Samanta, *Phys. Rev. C* **47**, 2994 (1993).
- [34] L. Trache, A. Azhari, H. L. Clark, C. A. Gagliardi, Y.-W. Lui, A. M. Mukhamedzhanov, R. E. Tribble, and F. Carstoiu, *Phys. Rev. C* **61**, 024612 (2000).
- [35] O. F. Nemets, V. G. Neudachin, A. T. Rudchik, Yu. F. Smirnov, and Yu. M. Tchuvil'sky, *Nucleon Associations in Atomic Nuclei and Many-Nucleon Transfer Reactions* (Naukova Dumka, Kiev, 1988) [in Russian].
- [36] S. Cohen and D. Kurath, *Nucl. Phys. A* **101**, 1 (1967).